Journal of the European Ceramic Society **8** (1991) 355–363

Interrelation among Flaw Resistance, K^R-Curve Behavior and Thermal Shock Strength Degradation in Ceramics. I. Theoretical Considerations

H. E. Lutz & M. V. Swain

Department of Mechanical Engineering, University of Sydney, Sydney, NSW 2006, Australia

(Received 14 February 1991; accepted 22 April 1991)

Abstract

This paper presents a new concept by which both the K^R-curve behavior and thermal shock strength degradation of a ceramic material can be predicted simultaneously by applying the 'Vickers Indentation Strength in Bending (ISB)' method.

Diese Arbeit stellt ein neues Verfahren vor, das es erlaubt, sowohl das K^R-Kurvenverhalten als auch die Abnahme der Thermoschockbeständigkeit eines keramischen Werkstoffes simultan durch Anwendung der 'Vickers-eindruck-Biegefestigkeits-(ISB-)'-Methode vorherzusagen.

On rapporte ici un nouveau concept grâce auquel on peut prévoir simultanément le comportement de la courbe K^R et la résistance à la dégradation par choc thermique, par application de la méthode de résistance à la flexion par indentation Vickers (ISB).

1 Introduction

The interest in ceramic materials has been increasing because of their excellent resistance to wear, corrosion, chemical attack and high temperature creep. However, their applicability is limited because of their brittleness or limited crack-resistance behavior, and their considerable strength degradation upon severe thermal shock. In addition, the development of new ceramic composites is hindered by the high costs of preparation and testing. The measurement of crack-resistance and thermal shock behavior of ceramics is necessary to characterize the fracture behavior of the material under mechanical loading as well as under rapidly changing temperatures. Unfortunately these measurements are time-consuming and expensive. The testing procedure and the applicability of the results are discussed in more detail below.

The crack-resistance behavior or toughness behavior of ceramics is generally referred to as R- or K^R-curve behavior depending on whether the crack resistance or the toughness as a function of crack extension is considered. The R-curve test involves controlled crack propagation through the material under an applied load. The crack propagation should be initiated from a sharp precrack. With the knowledge of load, displacement and crack length, R or K^R can be evaluated using either the energy or stress-intensity concept. The Irwin relation, the energy release rate $G=(K^{R^2}/E)$, with E being the Young's modulus of the material, is only valid for linear-elastic behaving materials, i.e. the K^R-curve measured on a 'quasi-ductile' behaving material does not simultaneously represent its R-curve behavior.

Glass, glass-ceramics and most fine-grained ceramics exhibit no R-curve behavior, i.e. their R-curve is flat. R is constant and independent of the crack extension a. In recent years a number of short- and long-range contact- and zone-shielding mechanisms have been described,[1] such as transformation toughening, microcrack toughening, crack deflection and crack branching, toughening by bridging and load-carrying processes behind the crack tip, which produce a more or less pronounced R-curve behavior. Although there is no unique R-curve behavior for a material,[2] i.e. R is a function of crack and sample geometry, notch depth, sample size, measuring technique and evaluation method,[3,4] the R-curve provides significant information about the fracture behavior of ceramics.

Cook & Clarke[5] suggested that the K^R-curve

Journal of the European Ceramic Society 0955-2219/91/$3.50

could be represented by a power function, that is

$$K^R = K_0\left(\frac{a}{a_0}\right)^\tau \quad (1)$$

where K_0 is regarded as the base toughness of the material in the absence of any toughening mechanisms and the term a_0 as the spatial extent of the crack at which toughening begins. The slope of the power function, τ, can easily be evaluated by linear regression of a double-logarithmic plot of K^R versus a. The situation where $\tau = 0$ corresponds to constant toughness; $\tau > 0$ indicates a pronounced K^R-curve behavior. Although these authors chose a simplistic expression to describe the K^R-curve shape, it accounts for some characteristic features of such curves, as will be outlined in the accompanying paper.

The thermal shock behavior of ceramics is conventionally measured by quenching small beams from an elevated temperature into water at room temperature and measuring their retained strength, σ_R, or modulus of rupture, MOR. For $\Delta T > \Delta T_c$ rapidly growing cracks are thought to arrest either when all of the strain energy is converted into fracture surface energy (Hasselman thermoelastic approach[6,7]) or when the statistically defined stress intensity factor, K, becomes less than the critical stress intensity factor, K_c.[8] Following Hasselman,[6] a damage resistance parameter, R'''', can be calculated for any ceramic material with

$$R'''' = \frac{E\gamma_{eff}}{\sigma_B^2} \quad (2)$$

Since R'''' should be proportional to the retained strength, σ_R, when normalized to the initial strength of a material, σ_B, a correlation between the R-curve behavior and the thermal shock strength degradation can be derived semi-empirically by modifying eqn (2) to

$$\frac{\sigma_R}{\sigma_B} \sim R'''' \sim \frac{\gamma_{WOF}}{\gamma_{ic}} \quad (3)$$

where γ_{WOF} is the specific work of fracture required to extend a crack and γ_{ic} is the energy to initiate crack growth. For a flat R-curve γ_{WOF}/γ_{ic} has a minimum value of 1·0. The steeper the R-curve, the larger the ratio becomes and the less is the anticipated strength degradation. Although it has been shown that this relationship holds reasonably well for alumina,[9] Mg partially stabilized zirconia ceramics[10] and duplex ceramics,[11,12] this approach is very simplistic, because the elastic strain energy which has been used to derive eqn (2) is difficult to estimate. It generally depends on time, Young's modulus, thermal conductivity, thermal expansion, sample dimensions, thermal diffusivity, heat transfer, quenching temperature difference and the onset conditions for thermal fracture.[7] In addition, only a portion θ of the strain energy is converted into fracture surface energy, with θ being a function of the material, the component geometry, the fracture onset condition and the test ambience.[13] Modelling a radiation-heating thermal shock, Bradley[14] supposed θ to be half of the average strain energy when compared to the total strain energy.

Using the stress intensity concept, Evans & Charles[13] explored the behavior of relatively large precracks in thermal stress fields. Their approach is based on a fracture mechanics analysis of thermal shock fracture derived earlier by Evans.[8] The authors regarded that the most important stress intensification derives from thermal stresses associated with the non-uniform temperature distribution in the body. For convective heat transfer conditions these stresses can be described by the normalized parameters:[8]

$$\Omega = \frac{\sigma(1-\nu)}{E\alpha\Delta T} \quad (4)$$

$$\Theta = \frac{kt}{c\rho r_0^2} \quad (5)$$

$$\beta = \frac{r_0 h}{k} \quad (6)$$

where α is the linear thermal expansion coefficient, ν is Poisson's ratio, ΔT is the initial temperature difference between the body and the environment, t is the time after exposure to ΔT, k is the thermal conductivity, ρ is the density, c is the specific heat, h is the heat transfer coefficient, r_0 is the pertinent semi-dimension of the specimen, and β is the Biot modulus. On the basis of these terms the time variation of stresses can be generalized. With these stresses the stress intensity factor for a crack extending in this stress field can be calculated using Green's function. The stress intensity factor, K_{TS}, for a crack propagating in a spatially variant stress field, $\sigma(x)$, is given by[8]

$$K_{TS} = 2(a/\pi)^{0.5}\int_0^a \frac{\sigma(x)[1+f(x/a)]}{(a^2-x^2)^{1/2}}\,dx \quad (7)$$

where a is the crack length and

$$f(x/a) = (1-x/a) \times [0{\cdot}2945 - 0{\cdot}3912(x/a)^2 + 0{\cdot}7685(x/a)^4 - 0{\cdot}9942(x/a)^6 + 0{\cdot}5094(x/a)^8] \quad (8)$$

Substituting σ from eqn (4) and normalizing the

length parameters gives the normalized stress intensity factor:

$$\kappa = \frac{K_{TS}(1-\nu)}{E\alpha\,\Delta T\sqrt{r_0}}$$

$$= 2(a/\pi r_0)^{0\cdot5}\int_0^1 \frac{\Omega(x/r_0)[1+f(x/a)]}{[1-(x/a)^2]^{0\cdot5}}\,\mathrm{d}(x/a) \qquad (9)$$

On the basis of the time (Θ in eqn (5)) and with the extension of this concept using finite element analysis it is possible to construct an envelope of the maximum κ with crack depth for a value of $\beta = 15$, which is typical for thermal shocking into water.[13-17] With a knowledge of κ, K_{TS} may be calculated as a function of ΔT, Young's modulus, E, and the crack depth (a/w), with $w = 2r_0$ being the sample thickness. In the case of a severe thermal shock a crack will propagate as long as K_{TS} exceeds the toughness of the material, K^R, and arrests at a certain crack length (a/w) for $K_{TS} \leq K^R$.

It is well known that the stress–strain behavior of many coarse microstructured or low-strength materials deviate from linear elasticity, as is schematically shown in Fig. 1. In addition, this deviation becomes larger the more the material is strained. Since the slope of a stress–strain curve reflects the Young's modulus E of the material, E can be reduced significantly with increasing strain, ε. As has been pointed out by Swain,[17] this effect is due to stress-induced microcracking and can lead to a tremendous reduction of K_{TS} under thermal shock. The author used the Iljuschin function[18]

$$E(\varepsilon) = E_0[1-\omega(\varepsilon)] \qquad (10)$$

to estimate the reduction of the secant and tangent modulus E, which can be calculated as the secant or tangential slope for any point of the stress–strain curve as a function of the strain ε. E_0 is the dynamic Young's modulus and ω is a damage parameter for quasi-plasticity. As has been observed by Swain,[17] ω increases first with increasing ε up to about 0·1% and approaches asymptotically a maximum value for higher strains, ω_{max}, which can be as high as 0·9. This behavior is schematically illustrated in Fig. 2. Since local tensile strains will exceed 0·1% and exhibit a sharp gradient under severe thermal shock (or during fracture), E, and hence K_{TS}, is expected to be tremendously reduced under thermal stress fracture conditions. This has a considerable effect on the retained strength of a thermal shock damaged material.

The retained strength of the thermally shocked material may be estimated from the extent of the crack growth predicted above. The applied stress intensity factor for such a crack is considered similar to a single-edged notch bend (SENB) fracture mechanics test,[17] that is

$$K_A = Y(a/w)\sigma_R a^{0\cdot5}$$
$$= (w)^{0\cdot5}\sigma_R(a/w)^{0\cdot5}$$
$$\times [1\cdot99 - 0\cdot41(a/w) + 18\cdot7(a/w)^2$$
$$- 38\cdot48(a/w)^3 + 53\cdot85(a/w)^4] \qquad (11)$$

The failure criteria of the material in flexure is then dependent upon the conditions $K_A > K^R$ and $\mathrm{d}K_A/\mathrm{d}a \geq \mathrm{d}K^R/\mathrm{d}a$.

Using the Green's function method the crack growth due to severe thermal shocking, the anticipated strength degradation and the specimen size effect can be estimated. Whilst an analytical solution can only be calculated for small cracks, supposing a thermal stress that exists in the absence of a crack, for longer cracks K can only be obtained numerically. Since a long crack affects the compliance of a body, the introduction of a crack not only modifies

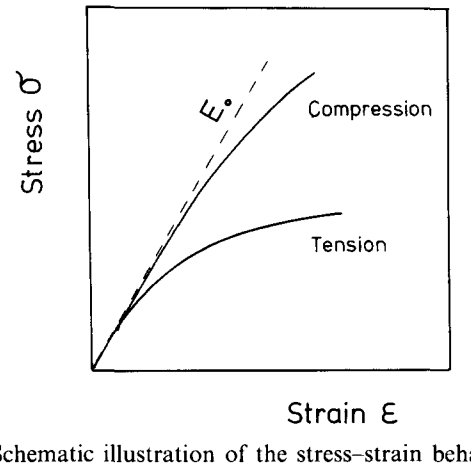

Fig. 1. Schematic illustration of the stress–strain behavior of quasi-ductile ceramics. The secant and tangent modulus E can be evaluated as a function of the strain for any point of the curve as the secantal and tangential slope.

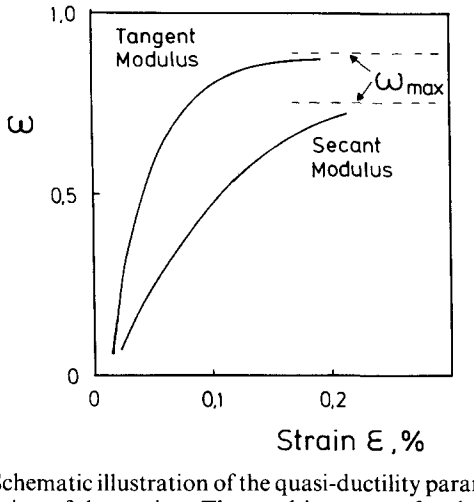

Fig. 2. Schematic illustration of the quasi-ductility parameter ω as a function of the strain ε. The resulting curves for the secant and tangent modulus can be calculated from the stress–strain curve in Fig. 1 using the Iljuschin function in eqn (10).

the local stress distribution but also reduces the stress level throughout the body.[13] In addition, as for the energy approach, the temperature sensitivity of the K^R-curve has not been taken into account. Although considerable work has been done to predict fracture upon severe thermal shock using energy and stress-intensity methods, the crack arrest predictions are still unsatisfactory.

The toughness of ceramics can be conveniently measured using the 'indentation strength in bending (ISB)' method.[19] According to this technique the retained strength of a sample is measured after damaging and introducing a crack in its surface by a Vickers indentation of a certain load, P_I. For very small loads, i.e. as long as the damage is smaller than the inherent flaw size, the strength is not reduced. For higher indentation loads, $P_I^2 > P_I^1$, however, the strength decreases from σ_I^1 to σ_I^2 with increasing load.[19] The strength decrease as a function of the Vickers indentation load of a material describes its 'flaw resistance'.

The influence of a material's R-curve on the contact or mechanical damage and resultant strength degradation has been considered in detail by Cook *et al.*[5,20] and Chantikul *et al.*[21] for the specific case of pointed indentation. These authors found that the extent of strength degradation was strongly influenced by the microstructure, which in turn determined the R-curve behavior. They investigated a range of alumina ceramics varying from single crystals through fine to coarser grained. As the grain size increased the initial strength decreased. However, increasing indentation loads lead to a higher retained strength for the coarser grained materials for indentation loads exceeding 100 N.

Cook & Clarke[5] suggested that the decrease in strength as a function of the Vickers indentation load can be described by the following expression:

$$\frac{\sigma_I^2}{\sigma_I^1} = \left[\frac{P_I^2}{P_I^1}\right]^{(2r-1)/(2r+3)} \tag{12}$$

This equation, which theoretically describes the quantitative relationship between the K^R-curve behavior and the 'flaw resistance' (or 'contact damage resistance, mechanical damage resistance'), is shown in Fig. 3 as a plot of $\log \sigma_I$ versus $\log P_I$. The slope of the resulting straight line contains τ. For $\tau = 0$ the absolute value of the slope is a maximum, with $\frac{1}{3}$ indicating that the material is 'flaw-sensitive'. With increasing τ the absolute value of the slope decreases approaching 0 at $\tau = 0{\cdot}5$, indicating 'ideal flaw tolerance'.

The advantage of the ISB method is that the initial crack length has been eliminated as a test variable

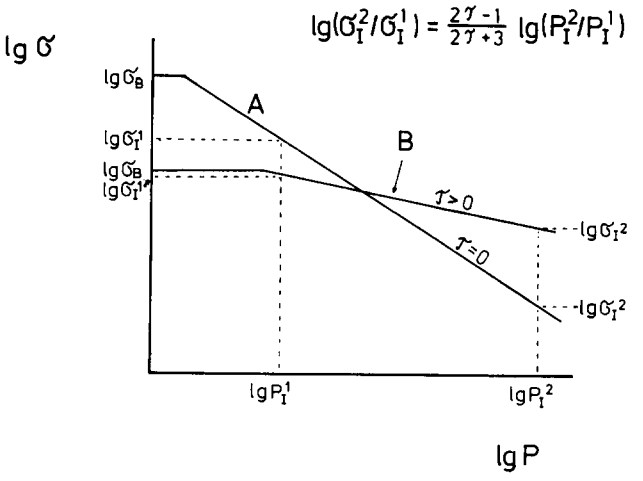

Fig. 3. Schematic illustration of the correlation between mechanical damage or flaw resistance and K^R-curve behavior. The logarithm of the strength is plotted versus the logarithm of the Vickers indentation load for two different materials with $\tau = 0$ and $\tau > 0$.

when compared to the direct crack measurement method in favor of an indentation load. In addition, the results are relatively insensitive to post-indentation slow crack growth phenomena. However, it has been considered important to establish that the radial crack evolution in any given test material is well behaved. An ill-defined crack pattern is most likely to appear when the initial crack length is comparable to the grain size of the material.[19] The presence of strong residual stresses is also considered to have a considerable influence on crack pattern[22] and crack propagation from the initial crack beneath the indentation.[23] It should be pointed out here that the derivation of eqn (12) is based on linear-elastic fracture mechanics.

As described above, two different correlations are already well known (Fig. 4). There is the correlation between the R-curve behavior and the thermal shock strength degradation on the one hand. It can either be simply described by the empirically derived proportionality in eqn (3) or calculated using the more sophisticated stress-intensity concept using eqns (9) and (11). However, the former has a strong specimen size dependence. On the other hand there is

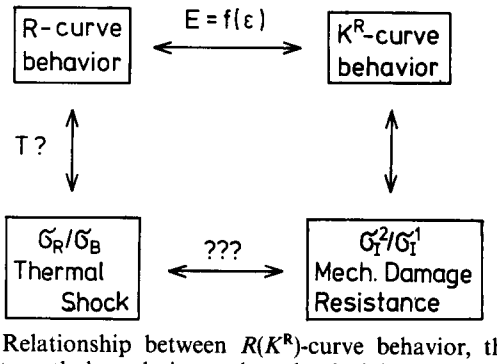

Fig. 4. Relationship between $R(K^R)$-curve behavior, thermal shock strength degradation and mechanical damage resistance.

the theoretically predicted correlation between the K^R-curve behavior and the flaw resistance described by eqn (12), which is based on the assumption that the materials behave linear elastically and that any K^R-curve can simply be expressed in the form of a power function in eqn (1).

The aim of this work is to compare both correlations and to establish an interrelationship among all three properties. This would allow one to predict the K^R-curve behavior and the thermal shock strength degradation simultaneously by the simple application of the ISB method.

2 Theoretical Considerations

2.1 Influence of temperature and quasi-plasticity

Temperature and quasi-plastic behavior which are observed in some ceramics doubtless have a non-neglectable influence on the K^R-curve behavior. Little work has been done to evaluate their quantitative effect. Here a rather simplistic approach is presented to account for their influence.

The increase in toughness of a ceramic exhibiting K^R-curve behavior is caused by energy-dissipating mechanisms about the crack tip or load-carrying processes behind the crack tip, which are in most ceramics activated by residual stresses. These stresses develop upon cooling after fabrication below a certain temperature, T^*. In most ceramics these stresses are either due to thermal expansion anisotropy among the grains of single-phase materials or due to thermal expansion mismatch in polyphase materials. In ZrO_2-containing ceramics the stress-induced tetragonal to monoclinic phase transformation of the ZrO_2 particles creates additional stresses. Starting at T^*, where the first residual stresses occur either spontaneously or induced by applied stresses (ZrO_2 phase transformation), these residual stresses are expected to increase linearly with decreasing temperature. To account for this temperature dependence of residual stresses it is assumed here that the K^R-curve slope τ depends in a very simple manner, i.e. linearly, on temperature T. As shown in Fig. 5, τ should be 0 at T^* and is thought to increase with decreasing temperature following the relationship

$$\tau = \tau_0\left(\frac{T-T^*}{R_T-T^*}\right) = d\tau_0 \qquad (13)$$

where τ_0 is the value of τ at room temperature, R_T.

It is apparent that most ceramics which exhibit a pronounced R-curve behavior also display 'quasi-ductility', that is an increasing deviation from linear

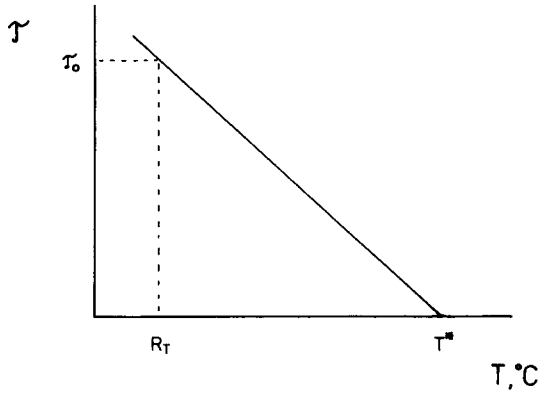

Fig. 5. Assumed relationship between τ and T.

elasticity with increasing strain (Fig. 1). For many of these ceramics this is caused by stress-induced microcracking and is, hence, an indicator for the presence of residual stresses. Alternatively, this non-linear stress–strain behavior is a consequence of the transformation toughening in metastable ZrO_2 microstructures. Although stress-induced microcracking has a minor toughening effect,[24] it seems to accompany other important toughening mechanisms, such as crack deflection, crack branching, crack bridging or frictional effects in the crack wake region, which are responsible for a pronounced K^R-curve behavior. The observation of quasi-ductility and R-curve behavior suggests there may exist a relationship between these events. As illustrated in eqn (1), the K^R-curve may be conventionally characterized by τ, whereas the stress–strain non-linearity is characterized by ω, as illustrated in eqn (10). Since ω is an indicator of the presence of residual stresses and since the residual stresses decrease with increasing temperature, ω is thought to decrease with increasing temperature and to be zero at T^*, and hence shows a similar behavior with T as τ. That indeed there is a relationship between τ_0 and ω_{max}, the maximum ω-value observed for very high strains (Fig. 2), is shown in Fig. 6, which plots

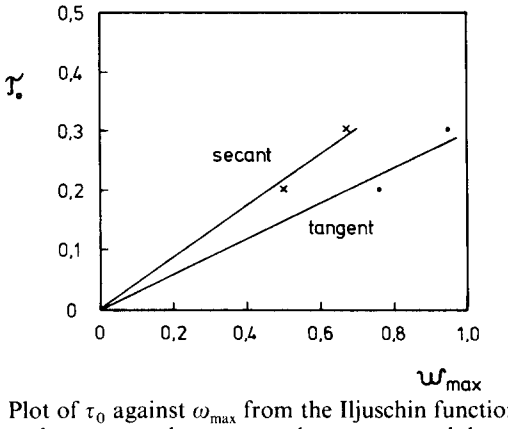

Fig. 6. Plot of τ_0 against ω_{max} from the Iljuschin function (eqn (10)) for the measured secant and tangent modulus of an alumina-zirconia and a titanium diboride composite obtained from papers of Swain[17] and Bannister & Swain.[25]

both terms for two ceramics, an alumina-zirconia and a titanium diboride composite, previously measured by Swain[17] and Bannister & Swain.[25] The authors measured E as the secant and tangential slope of the stress–strain curve and calculated ω as a function of ε (Fig. 2). Since brittle ceramics show no R-curve behavior, $\tau_0 = 0$ for $\omega_{max} = 0$. It is probable that τ_0 increases steeply when ω_{max} approaches 1·0 following a steep curvature. The data points, however, allow us to postulate a linear relationship within the range $0 \geq \omega_{max} \geq 0{\cdot}7$ and 0·9 for the secant and tangent values, respectively, with $\tau_0 \approx 0{\cdot}3\omega_{max}$ for the tangent values.

2.2 K^R-curve behavior and thermal shock strength degradation

For simplicity, we assume here that the expression in eqn (3) empirically derived from the Hasselman thermoelastic approach describes the relationship between the R-curve behavior and the thermal shock strength degradation tolerably well. In an endeavor to more adequately relate this to the observed K^R-curve behavior as well as the temperature sensitivity of this feature the expression in eqn (3) is modified by the Irwin stress intensity factor equivalent, namely

$$\frac{\sigma_R}{\sigma_B} \sim \frac{\gamma_{WOF}}{\gamma_{ic}} = \frac{K_{eff}^{R^2} E_0}{K_0^{R^2} E_{eff}(\varepsilon, T)} \tag{14}$$

where K_{eff}^R and $E_{eff}(\varepsilon, T)$ are average values for toughness and Young's modulus, respectively, between a_0 and a certain crack length, a. An estimate of K_{eff}^R may be found by integration of eqn (1) with $\tau = d\tau_0$:

$$K_{eff}^R = \frac{1}{(a - a_0)} \int_{a_0}^{a} \left[K_0 \left(\frac{a}{a_0} \right)^{d\tau_0} \right] da \tag{15}$$

with the temperature dependence of the effective E modulus given by

$$E_{eff}(\varepsilon, T) = E_0(1 - \omega_{eff}(\varepsilon, T)) \tag{16}$$

ω_{eff} is the mean value between $\varepsilon = 0$ and the maximum value which appears under severe thermal shock strain. Its value is not known but can be approximately estimated.

With eqns (15) and (16) the correlation between the K^R-curve behavior and the thermal shock strength degradation in eqn (14) is then given by the expression

$$\frac{\sigma_R}{\sigma_B} \sim \frac{1}{(1 - \omega_{eff})} \frac{1}{(1 + d\tau_0)^2} \frac{(a^{d\tau_0 + 1} - a_0^{d\tau_0 + 1})^2}{a_0^{2d\tau_0}(a - a_0)} \tag{17}$$

Since a_0 is very small when compared to a, eqn (17) can be simplified to

$$\frac{\sigma_R}{\sigma_B} \sim \frac{1}{(1 - \omega_{eff})} \frac{1}{(1 + d\tau_0)^2} \left(\frac{a}{a_0} \right)^{2d\tau_0} \tag{18}$$

For a direct comparison of the relationship between (σ_R/σ_B) and τ_0 with the relationship between (σ_I^2/σ_I^1) and τ_0 of eqn (12) above proportionality has to be calibrated. As σ_R/σ_B can never exceed 1·0 it is arbitrarily assumed here that this maximum value is reached for $\tau_0 = 0{\cdot}5$, $d = 1{\cdot}0$ and $\omega_{eff} = 0$. It is possible to show that the above conditions are met when multiplying eqn (18) by a factor $c = 2{\cdot}25(a/a_0)^{-1}$, which modifies eqn (18) to

$$\frac{\sigma_R}{\sigma_B} = \frac{1}{(1 - \omega_{eff})} \frac{2{\cdot}25}{(1 + d\tau_0)^2} \left(\frac{a}{a_0} \right)^{(2d\tau_0 - 1)} \tag{19}$$

2.3 Correlation between flaw resistance and thermal shock strength degradation

The correlation between K^R-curve behavior and thermal shock strength degradation described by eqn (19) may now be compared with the relationship between the flaw resistance and the K^R-curve behavior, which is characterized by eqn (12).

First of all, it is assumed that the material displays ideal linear-elastic behavior, i.e. $\omega_{eff} = 0$, and that its K^R-curve is not influenced by temperature during thermal shock, i.e. $d = 1$. Equation (19), which can be simplified under the above conditions, is now compared with eqn (12). Both have been calculated for (a/a_0) and $(P_I^2/P_I^1) = 10$ and 50, and plotted as a function of τ_0. As is shown in Fig. 7(a), eqn (12) (solid curves) and eqn (19) (broken curves) result in similar curves. The retained strength after both a surface indentation damage or a severe thermal shock increases with increasing τ. The larger the considered range of the Vickers indentation load and the crack extension, i.e. the larger the ratios (P_I^2/P_I^1) and (a/a_0), the smaller is the retained strength and the more it is affected by an increase in τ.

Figure 7(b) shows the influence of temperature and quasi-plasticity on the curvature of eqn (19) for $(a/a_0) = 25$ when compared to eqn (12), with $(P_I^2/P_I^1) = 25$ shown by curve 1. If τ is temperature-independent and $\omega_{eff} = 0$, the retained strength steeply increases with increasing τ, as can be seen from curve 2. A reduction of τ by temperature (with $\omega_{eff} = 0$) reduces the retained strength the higher τ is. This is apparent from curve 3 for a 50% reduction of τ. For $\omega_{eff} > 0$, but being independent of τ, simply results in an increase of curve 3 by a constant factor. However, it is more likely that an increase in τ is accompanied by an increase in ω_{eff}, as has been

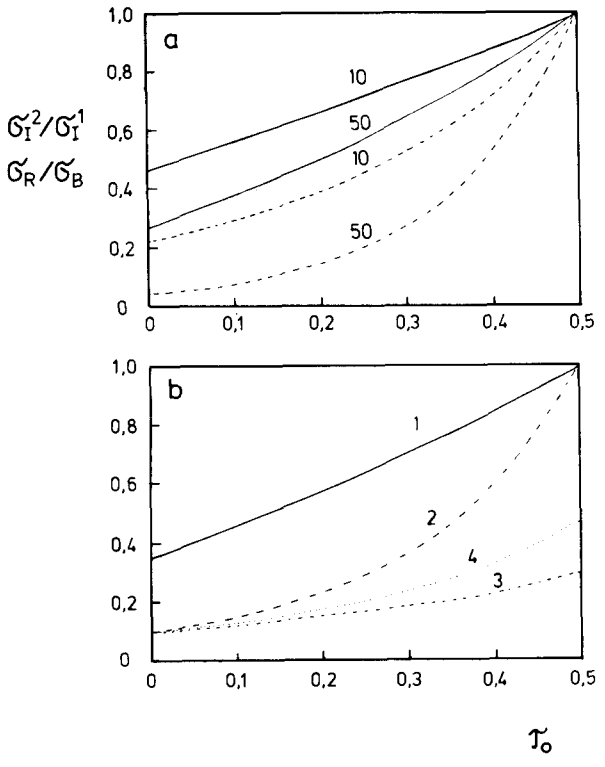

Fig. 7. Plots of σ_R/σ_B and σ_I^2/σ_I^1, respectively, versus τ: (a) eqn (12) (solid curves) and eqn (19) (broken curves) are shown for (P_I^2/P_I^1) and $(a/a_0) = 10$ and 50, respectively; (b) eqn (12) (curve 1) is compared with eqn (19) for (P_I^2/P_I^1) and $(a/a_0) = 25$, assuming that $d = 1$, $\omega_{eff} = 0$ (curve 2); $d = 0{\cdot}5$, $\omega_{eff} = 0$ (curve 3); and $d = 0{\cdot}5$, $\omega_{eff} = 0{\cdot}5\omega_{max} = 0{\cdot}5 \times 3{\cdot}2\tau = 0{\cdot}5 \times 3{\cdot}2 \times 0{\cdot}5\tau_0$ (curve 4).

outlined in Section 2.1. Assuming that $\omega_{eff} = 1/2\omega_{max}$, $\omega_{max} \approx 3{\cdot}2\tau$ (estimated from the tangential values in Fig. 6) and $\tau = 1/2\tau_0$ (50% reduced) leads to curve 4. It is apparent that temperature and quasi-plasticity are counteracting effects which cannot be neglected. A comparison of the curve shows, however, that the main tendency, the increase in the retained strength with increasing τ, is not affected. It is remarkable that curve 4 exhibits a more similar curvature compared to curve 1 than curves 2 and 3 show. Despite the quantitative difference the qualitative similarity of curves 1 and 4 indicates that mechanical and thermal shock strength degradation are similarly influenced by the *R*-curve behavior. It is supposed that as a consequence both the *R*-curve behavior and the thermal shock strength degradation of ceramics may be estimated on the basis of mechanical damage behavior.

2.4 Green's function method

The correlation between the K^R-curve behavior and the thermal shock strength degradation can alternatively be derived by using a fracture mechanics analysis of cracking due to severe thermal shock which has been made by Evans & Charles,[13] as has been mentioned in the introduction. It is possible to

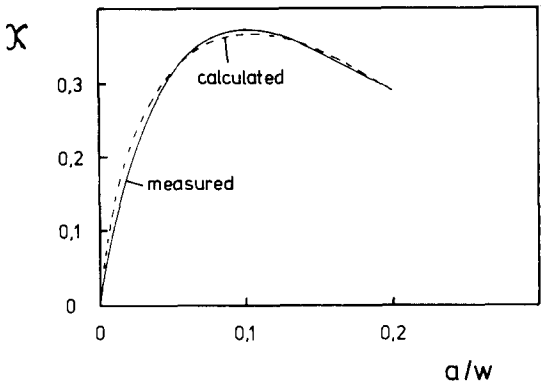

Fig. 8. Comparison of the constructed[13–17] κ-envelope with eqn (20).

construct an envelope of κ to predict the crack arrest conditions for thermal shocking into water.[13–16] Substituting r_0 of eqn (9) by the width $w = 2r_0$ of the specimen this κ-envelope can be approximately described by the function

$$\kappa = 1{\cdot}3945(a/w)^{0{\cdot}46} - 5{\cdot}322(a/w)^{1{\cdot}64} \qquad (20)$$

In Fig. 8 the constructed envelope is compared with the plot of eqn (20). With eqn (9) K_{TS} is then given by

$$K_{TS} = \frac{E_0(1 - \omega_{max})\alpha\,\Delta T(w/2)^{0{\cdot}5}}{(1 - \nu)} \times [1{\cdot}3945(a/w)^{0{\cdot}46} - 5{\cdot}322(a/w)^{1{\cdot}64}] \qquad (21)$$

In the case of a severe thermal shock a crack will propagate as long as $K_{TS} \geq K^R$ with (eqn (1) written as function of (a/w))

$$K^R = K_0(a_0/w)^{-d\tau_0}(a/w)^{d\tau_0} = c(a/w)^{d\tau_0} \qquad (22)$$

and arrest at a certain (a/w) for $K_{TS} \leq K^R$, which is given by the intersection of the K_{TS}-curve with the superimposed K^R-curve.

With a knowledge of the K^R-curve behavior of a ceramic the retained strength of the material after severe thermal shock, σ_R/σ_B, can be estimated as a function of $K^R(T)$, $E(\omega_{eff})$ and ΔT using the following procedure, which is graphically illustrated in Fig. 9.

As a first step the slope of the measured K^R-curve, τ_0, is graphically determined. The data points are plotted on a double-logarithmic diagram. The slope of the straight line through all data points which is obtained by linear regression equals τ_0. The intersection of the straight line with the *Y*-axis gives *c*. This has been performed for an alumina-zirconia ceramic described in detail by Garvie *et al.*[26] The linear regression of the $\ln(K^R)$ versus $\ln(a)$ plot gives $\tau_0 = 0{\cdot}306$. From Fig. 10 it is obvious that the calculated K^R-curve is in good agreement when compared to the measured K^R-curve.

During thermal shock the K^R-curve slope is thought to be reduced by a factor *d*. The value of *d*

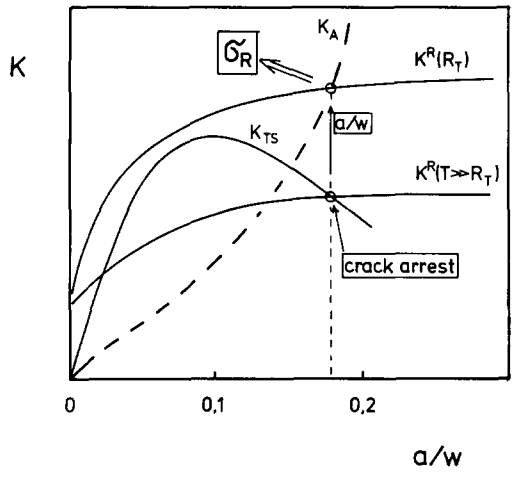

Fig. 9. Schematic illustration of the thermal-shock generated stress intensity factor, K_{TS}, and a temperature-influenced K^R-curve, which are given by eqns (21) and (22), respectively. The intersection of the two curves gives the crack depth (a/w). Superimposed are the room-temperature K^R-curve (eqn (22)) and the applied stress-intensity factor K_A, which can be calculated with eqn (11) using the (a/w)-value.

can be estimated using eqn (13), assuming that cracks which are initiated during the thermal shock event propagate through material which is still at furnace temperature. For the alumina-zirconia ceramic the lowest temperature where no stresses occur, T^*, has been assumed to be 1200°C. Equation (13) then gives d-values of 0·5 and 0·167 for quenches over temperature differences of 600 and 1000°C, respectively.

The value of (a/w) for crack arrest may now be calculated from the intersection point of the K_{TS}-curve (eqn (21)) with the temperature-reduced K^R-curve (eqn (22)), as is shown in Fig. 9. For the calculation of the K_{TS}-curve it is necessary to estimate ω_{eff}. According to the slope of the straight line through the tangential plots in Fig. 6 ω_{max} is approximately $3{\cdot}2\tau$.

The anticipated retained strength at room temperature is finally obtained by inserting the crack

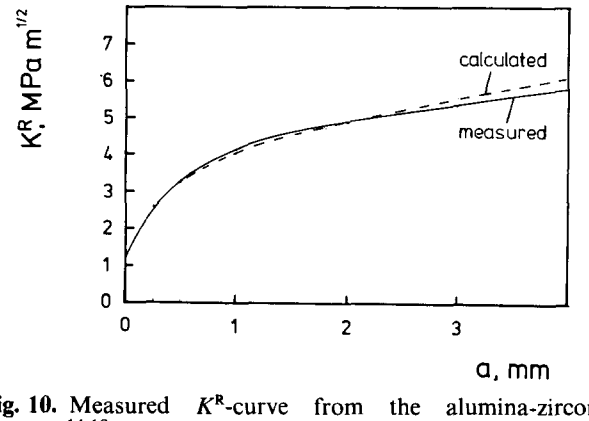

Fig. 10. Measured K^R-curve from the alumina-zirconia material[14,18] when compared to the approximated curve, which can be calculated using eqns (1) or (22).

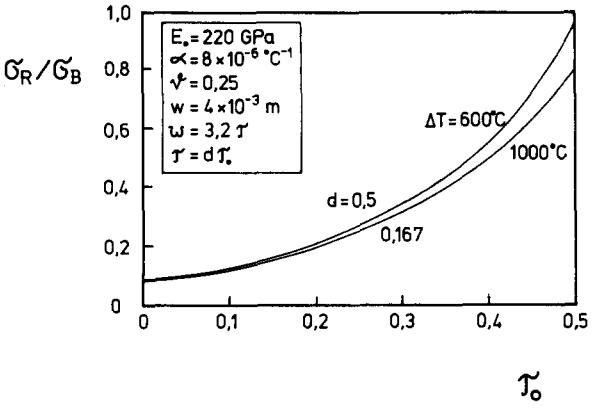

Fig. 11. Plot of σ_R/σ_B versus τ calculated by eqns (21), (22) and (11) for $\Delta T = 600$ and 1000°C.

arrest value (a/w) and the corresponding room temperature value of K^R in eqn (11) (see Fig. 9).

In Fig. 11 σ_R/σ_B of the alumina-zirconia ceramic is plotted versus τ for $\Delta T = 600$ and 1000°C. A comparison of these curves with the curves in Fig. 7 indicates that the relationship between the K^R-curve behavior and the thermal shock strength degradation, if derived by the Green's function method or based on the Hasselman thermoelastic approach, are quite similar. However, the above calculation results in a much lower σ_R/σ_B ratio (0·355 and 0·336 for $\Delta T = 600$ and 1000°C) for the alumina-zirconia ceramic when compared to the experimental results (0·81 and 0·73) from Garvie *et al.*,[26] indicating that the temperature influence may be overestimated. The resulting curves in Figs 7 and 11, nevertheless, support the assumption of an approximate proportionality between mechanical damage resistance and thermal shock strength degradation.

In the accompanying paper[27] flaw resistance, K^R-curve behavior and thermal shock behavior of different ceramics are investigated. The interrelation between all three properties is analysed and compared with the theoretical considerations in this paper.

3 Conclusions

The correlation between the toughness behavior (K^R-curve behavior) and the thermal shock strength degradation and the relationship between the toughness behavior and the flaw resistance show interesting similarities, which makes it possible to establish a semi-quantitative relationship between all three properties. This may be used to predict toughness behavior and thermal shock strength degradation of ceramics simultaneously with the knowledge of its flaw resistance alone.

Acknowledgements

One of the authors (H.E.L.) thanks the Deutsche Forschungsgemeinschaft, Bonn, West Germany, for financial support under contract number lu 416/1-1. N. Claussen and P. Greil are thanked for their assistance to make this project possible.

References

1. Ritchie, R. O., Mechanisms of fatigue crack propagation in metals, ceramics and composites: control of crack tip shielding. *Mater. Sci. Engng*, **A103** (1988) 15–28.
2. Marshall, D. B. & Swain, M. V., Crack-resistance curves in magnesia-partially stabilized zirconia. *J. Am. Ceram. Soc.*, **71**(6) (1988) 399–407.
3. Steinbrech, R., Knehans, R. & Schaarwaechter, W., Increase of crack resistance during slow crack growth in Al_2O_3 bend specimens. *J. Mater. Sci.*, **18** (1983) 265–70.
4. Swain, M. V., *R*-curve behavior in ceramic materials. In *Advanced Ceramics II*, ed. S. Somiya. Elsevier Applied Science, Barking, 1988, pp. 45–67.
5. Cook, R. F. & Clarke, D. R., Fracture stability, *R*-curves and strength variability. *Acta Met.*, **36**(3) (1988) 555–62.
6. Hasselman, D. P. H., Unified theory of fracture initiation and crack propagation in brittle ceramics. *J. Am. Ceram. Soc.*, **52**(11) (1969) 600–4.
7. Hasselman, D. P. H., Severe thermal environments figures of merit for thermal shock resistance of high temperature brittle materials. *Ceramurgia Int.*, **4** (1978) 147–51.
8. Evans, A. G., Thermal fracture in ceramic materials. *Proc. Brit. Ceram. Soc.*, **25** (1975) 217–35.
9. Homeny, J. & Bradt, R. C., Thermal shock of refractories. In *Thermal Stresses in Severe Environments*, ed. D. P. H. Hasselman & R. A. Heller. Plenum Press, New York, 1980, pp. 343–63.
10. Swain, M. V., *R*-curve behavior of magnesia–partially stabilized zirconia and its significance to thermal shock. In *Fracture Mechanics of Ceramics, Vol. 6*, ed. R. C. Bradt, A. G. Evans, D. P. H. Hasselman & F. F. Lange. Plenum Press, New York, 1983, pp. 345–59.
11. Lutz, H. E., Claussen, N. & Swain, M. V., K^R-curve behavior of duplex-ceramics. *J. Am. Ceram. Soc.*, **74**(1) (1991) 11–18.
12. Lutz, H. E., Swain, M. V. & Claussen, N., Thermal shock behavior of duplex-ceramics. *J. Am. Ceram. Soc.*, **74**(1) (1991) 19–24.
13. Evans, A. G. & Charles, E. A., Structural integrity in severe thermal environments. *J. Am. Ceram. Soc.*, **60**(1–2) (1977) 22–8.
14. Bradley, F., Thermoelastic analysis of radiation-heating thermal shock. *High Temp. Technol.*, **6**(2) (1988) 63–72.
15. Emery, A. F., Stress-intensity factors for thermal stresses in thick hollow cylinders. *J. Basic Engng, Trans. ASME*, **88**(1) (1966) 45–53.
16. Trantina, G. G. & Roberts, J. T. A., Crack propagation in a thermally stressed ceramic reactor fuel. In *Fracture Mechanics of Ceramics, Vol. 2*, ed. R. C. Bradt, D. P. H. Hasselman & F. F. Lange. Plenum Press, New York, 1973, pp. 779–90.
17. Swain, M. V., *R*-curve behavior and thermal shock resistance of ceramics. *J. Am. Ceram. Soc.*, **73**(3) (1990) 621–8.
18. Iljuschin, A. A., Plastichnost. In *OGIZ GITTL*, Moscow, 1948, p. 16.
19. Chantikul, P., Anstis, G. R., Lawn, B. R. & Marshall, D. B., A critical evaluation of indentation techniques for measuring fracture toughness. II: Strength method. *J. Am. Ceram. Soc.*, **14**(9) (1981) 539–43.
20. Cook, R. F., Lawn, B. R. & Fairbanks, C. J., Microstructure-strength properties in ceramics. I: Effect of crack size on toughness. *J. Am. Ceram. Soc.*, **68** (1985) 604–15.
21. Chantikul, P., Bennison, S. J. & Lawn, B. R., Role of grain size in the strength and *R*-curve properties of alumina. *J. Am. Ceram. Soc.*, **73**(8) (1990) 2419–27.
22. Tandon, R., Green, D. J. & Cook, R. F., Surface stress effects on indentation fracture sequences. *J. Am. Ceram. Soc.*, **73**(9) (1990) 2619–27.
23. Lai, T. R., Hogg, C. L. & Swain, M. V., Comparison of fracture toughness determination of Y-TZP materials using various testing techniques. In *Ceramic Developments*, ed. C. C. Sorrell & B. Ben-Nissan. Materials Science Forum Vols 34–36, Trans. Tech. Publications Ltd, Switzerland, 1988, pp. 1071–5.
24. Evans, A. G. & Faber, K. T., Crack growth resistance of microcracking brittle materials. *J. Am. Ceram. Soc.*, **67**(4) (1984) 255–60.
25. Bannister, M. K. & Swain, M. V., Thermal shock of a titanium di-boride composite. *Ceram. Int.*, **16** (1990), 77–83.
26. Garvie, R. C., Goss, M. F., Marshall, S. & Urbani, C., Dense, thermal shock resistant advanced refractories. In *Proc. Adv. Refract. Met. Ind., Vol. 4*, ed. M. A. J. Rigand. Pergamon Press, New York, 1987, pp. 53–69.
27. Lutz, H. E. & Swain, M. V., Interrelation among flaw resistance, K^R-curve behavior and thermal shock strength degradation in ceramics—II. Experiment. *J. Europ. Ceram. Soc.*, **8** (1991) 365–74.